Journal of Biomolecular NMR, 10 (1997) 403–408
KLUWER/ESCOM

J-Bio NMR 515

Determination of backbone nitrogen–nitrogen J correlations in proteins

Karsten Theis[a], Andrew J. Dingley[a], Astrid Hoffmann[b], James G. Omichinski[b] and Stephan Grzesiek[a,b,*]

[a]*Institute of Physical Biology, Heinrich-Heine-Universität, D-40225 Düsseldorf, Germany*
[b]*IBI-2, Institute of Structural Biology, Forschungszentrum Jülich, D-52425 Jülich, Germany*

Received 14 October 1997
Accepted 30 October 1997

Keywords: Nitrogen–nitrogen J coupling; HOHAHA; TOCSY; ψ Angle; Relaxation; Ubiquitin

Summary

Recently, a quantitative J correlation technique has been presented which makes use of homonuclear Hartmann–Hahn cross-polarization (TOCSY) to measure $^3J_{C'C'}$ in proteins isotopically enriched with ^{13}C [Grzesiek, S. and Bax, A. (1997) *J. Biomol. NMR*, **9**, 207–211]. Since homonuclear Hartmann–Hahn is twice as fast as conventional COSY transfer, this method is much less sensitive to transverse relaxation, which is the principal limiting factor in achieving long-range J-coupling correlations in macromolecules. Here we describe a similar experiment which is used to measure $^3J_{NN}$ coupling constants between sequential amide ^{15}N nuclei in the backbone of ubiquitin. As expected from the low magnetic moment of ^{15}N, the $^3J_{NN}$ coupling constants are exceedingly small, with values between 0.14 and 0.36 Hz for residues in β-conformations and values below 0.15 Hz for residues in α-conformations. In contrast to what is expected from a Karplus-type dependence on the backbone angle ψ, large differences in the values of $^3J_{NN}$ are observed for a number of residues with very similar backbone ψ angles. A quantitative description of statistical and systematic errors, in particular of relaxation effects during the TOCSY transfer, shows that these differences are highly significant.

Characterization of the backbone angle ϕ by the measurement of one or several of the six different three-bond J-couplings ($^3J_{HNH\alpha}$, $^3J_{HNC\beta}$, $^3J_{HNC'}$, $^3J_{C'H\alpha}$, $^3J_{C'C\beta}$, and $^3J_{C'C'}$) has become a routine tool for three-dimensional structure determination of proteins (Bystrov, 1976; DeMarco et al., 1978; Pardi et al., 1984; Wüthrich, 1986; Ludvigsen et al., 1991; Schmieder et al., 1992; Garrett et al., 1994; Seip et al., 1994; Weisemann et al., 1994; Wang and Bax, 1995, 1996; Hu and Bax, 1996). In principle, the backbone angle ψ is characterized by the following three-bond J-couplings: $^3J_{C\beta N}$, $^3J_{H\alpha N}$, and $^3J_{NN}$. In practice, these coupling constants are rather small due to the low gyromagnetic ratio of the ^{15}N nucleus and they are therefore difficult to measure in larger polypeptides, where frequency resolution or magnetization transfer is limited by fast transverse relaxation. Only recently, a Karplus relation for one of these couplings ($^3J_{H\alpha N}$) has been determined experimentally (Wang and Bax, 1995).

Magnetization transfer in homonuclear Hartmann–Hahn mixing (TOCSY) schemes occurs twice as fast as in pulse-interrupted free precession (Braunschweiler and Ernst, 1983; Bax and Davis, 1985; Schleucher et al., 1996). This higher rate can be used to increase the sensitivity of quantitative J-correlation experiments for biomacromolecules with larger rotational correlation times. This principle has been applied in the (HN)CO(CO)NH experiment, where measurement of $^3J_{C'C'}$ couplings in the range of 1 Hz is possible even for a protein with a rotational correlation time of ~12 ns (Grzesiek and Bax, 1997). Due to their even smaller size, sequential $^3J_{NN}$ couplings have been very difficult to detect with conventional techniques even for smaller proteins such as human ubiquitin with a correlation time of 4 ns. In this communication, we use the sensitivity enhancement by the homonuclear TOCSY transfer to characterize the sequential $^3J_{NN}$ couplings in this protein and give a quantitative description of the systematic errors induced by relaxation effects during the extended TOCSY mixing period.

The scheme in Fig. 1 consists of a refocused ^1H-^{15}N

*To whom correspondence should be addressed at: IBI-2, Institute of Structural Biology, Forschungszentrum Jülich, D-52425 Jülich, Germany.

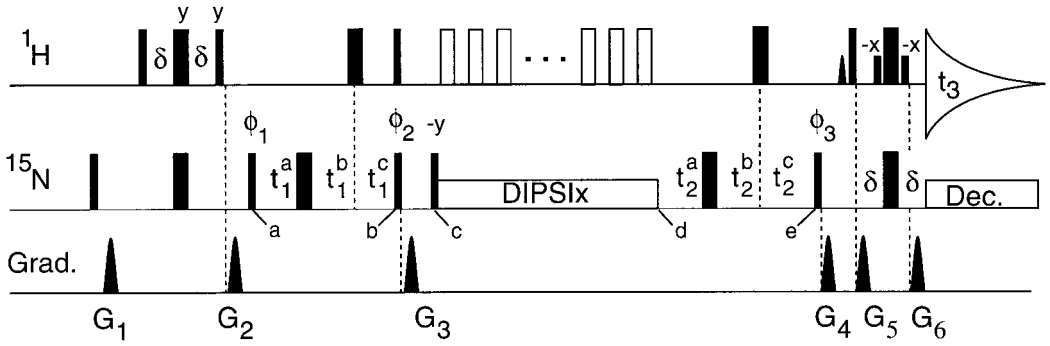

Fig. 1. Pulse sequence of the 3D (H)NNH-TOCSY experiment. Narrow and wide pulses denote 90° and 180° flip angles, respectively, and unless indicated otherwise the phase is x. ^{1}H and ^{15}N carrier positions are on the H_2O resonance and at 118 ppm, respectively. Rectangular low-power ^{1}H pulses are applied using $\gamma_H B_1 = 200$ Hz. The shaped 90°_{x} pulse has a sine-bell amplitude profile and a duration of 3.1 ms. All regular ^{15}N pulses are applied at an rf field strength $\gamma_N B_2 = 5.6$ kHz, whereas the ^{15}N decoupling is applied at an rf field strength of $\gamma_N B_2 = 1.25$ kHz. DIPSI$_x$ refers to the application of isotropic mixing, using the DIPSI-2 (Shaka et al., 1988) mixing scheme, with the rf field ($\gamma_N B_2 = 2.8$ kHz) applied along the ±x axis. Delay durations: $\delta = 2.25$ ms; $t_1^a(n_1) = 2.25$ ms $- n_1 * 0.08$ ms; $t_1^b(n_1) = n_1 * 0.52$ ms; $t_1^c(n_1) = 2.25$ ms $+ n_1 * 0.6$ ms; $n_1 = 0, 1, ..., 26$; $t_2^a(n_2) = 2.25$ ms $- n_2 * 0.08$ ms; $t_2^b(n_2) = n_2 * 0.52$ ms; $t_2^c(n_2) = 2.25$ ms $+ n_2 * 0.6$ ms; $n_2 = 0, 1, ..., 26$; Phase cycling: $\phi_1 = x,-x$; $\phi_2 = 2(y),2(-y)$; $\phi_3 = 4(x),4(-x)$; receiver = x,2(–x),x,–x,2(x),–x. Quadrature detection in the t_1 and t_2 dimensions is obtained by altering ϕ_1 and ϕ_3 in the States-TPPI manner, respectively. Gradients (sine-bell shaped; 25 G/cm at center): $G_{1,2,3,4,5,6} = 2$, 2.5, 6, 1.0, 0.4, and 0.4 ms.

HSQC experiment, where magnetization transfer between sequential amide ^{15}N nuclei is achieved by the insertion of a DIPSI-2 mixing sequence. Magnetization is transferred from an amide proton $^{1}H^{Ni}$ onto its attached $^{15}N^{i}$ nucleus (time point *a*). During a ^{15}N semi-constant time evolution period, this nitrogen–proton antiphase magnetization is refocused into in-phase magnetization of the nucleus N^i (time point *b*) and the frequency of nucleus N^i is measured (t_1). After a z-filter between time points *b* and *c*, N_x^i-magnetization is subjected to the DIPSI-2 isotropic mixing sequence (Shaka et al., 1988). At the beginning of every DIPSI-2 cycle (i.e. approximately every 5 ms), a ^{1}H 180° pulse is applied in order to invert the proton $|\alpha>$ and $|\beta>$ spin states. This serves to eliminate differential relaxation of the ^{15}N doublet caused by dipolar/CSA cross-correlation (Goldman, 1984; Boyd et al., 1990; Kay et al., 1992). During the mixing period, a fraction of the magnetization is transferred into N_x^{i+1} or N_x^{i-1} depending on the value of $^{3}J_{NiNi+1}$ and $^{3}J_{NiNi-1}$, while another fraction of the magnetization remains as N_x^i. The frequency of the N_x^i, N_x^{i+1} or N_x^{i-1} nuclei is then measured in the second ^{15}N semi-constant time evolution period (t_2) between time points *d* and *e*. At the end of this interval, the magnetization is defocused into antiphase proton magnetization, such that the relevant spin operator terms $2N_y^iH_z^i$, $2N_y^{i+1}H_z^{i+1}$, and $2N_y^{i-1}H_z^{i-1}$ at time point *e* can be refocused into proton in-phase magnetization H_x^i, H_x^{i+1}, or H_x^{i-1} at the beginning of the proton detection period (t_3). In the three-dimensional experiment, this sequence gives rise to observable resonances at the frequencies (ω^{Ni}, ω^{Nj}, ω^{Hj}) where i = j–1, j, or j+1, and we therefore name the experiment (H)NNH-TOCSY.

Neglecting, for the moment, effects of relaxation and the small additional transfer between the nitrogen nuclei during the semi-constant time evolution periods t_1 and t_2, the ratio of cross-peak intensity I_{ji} to diagonal-peak intensity I_{ii} is given by (Grzesiek and Bax, 1997):

$$I_{ji}/I_{ii} = [1 - \cos(2\pi J_{NjNi}\tau_m)] / [1 + \cos(2\pi J_{NjNi}\tau_m)] = \tan^2(\pi J_{NjNi}\tau_m) \quad (1)$$

In contrast to quantitative J-correlation experiments of the 'out-and-back' type, quantitative J-correlation experiments of the 'one-way' TOCSY type are not symmetrical. Losses of magnetization due to relaxation or pulse imperfection are therefore different for the periods before and after the TOCSY mixing. This leads to errors in the determination of the J-coupling constant according to Eq. 1. Such errors can be corrected when the value I_{ji}/I_{ii} in Eq. 1 is replaced by the geometric mean of the ratios of cross-peak to diagonal-peak intensities for the connectivities from residue i to j and j to i (Grzesiek and Bax, 1997):

$$[(I_{ji} \times I_{ij}) / (I_{ii} \times I_{jj})]^{1/2} = \tan^2(\pi J_{NjNi}\tau_m) \quad (2)$$

The pulse scheme is demonstrated on a sample of 1.5 mM ^{15}N-enriched human ubiquitin in a 220 µl Shigemi microcell at pH 4.7, 95% H_2O/5% D_2O. All measurements were carried out on a Bruker DMX600 spectrometer. In order to avoid problems associated with power dissipation during the extended ^{15}N mixing periods at a radio frequency field strength of 2.8 kHz, a double-resonance broadband inverse probe equipped with a z-gradient was used instead of the standard triple-resonance probe. The largest sensitivity for cross peaks in this experiment is achieved when the length of the ^{15}N-DIPSI mixing period is set to twice the length of the transverse ^{15}N relaxation time (Grzesiek and Bax, 1997). For non-mobile residues, ^{15}N transverse relaxation times of ubiquitin at 25 °C are approximately 170 ms (Tjandra et al., 1995). In order to

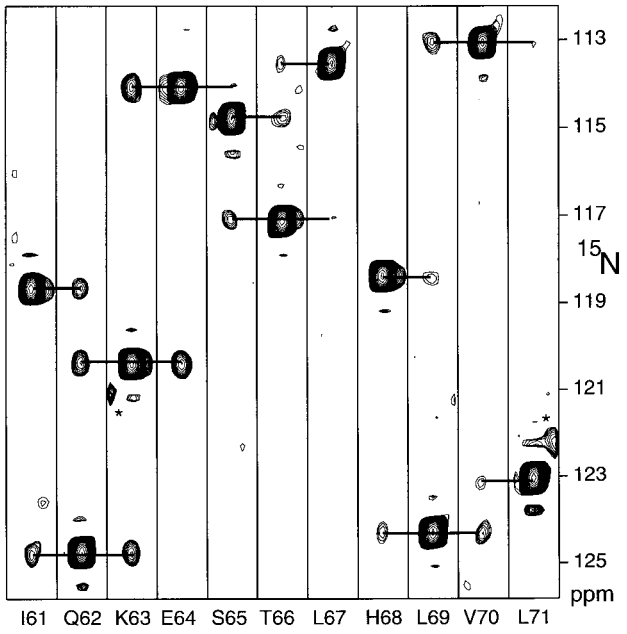

Fig. 2. (F1,F3) strips from the 3D (H)NNH-TOCSY spectrum of 1.5 mM ubiquitin (25 °C, 12 h experimental time), taken at the $^{1}H^{N}$ (F3) and ^{15}N (F2) frequencies of I61–L71. Correlations from residues with $^{1}H^{N}$ and ^{15}N shifts in the vicinity of the selected amide strip are marked '*'. Interresidue $N^{i}N^{i+/-1}$ connectivities are marked by horizontal lines.

reduce the power dissipation in the probe, mixing periods between 0.25 and 0.33 s were chosen as a compromise in the experiments. The 3D (H)NNH-TOCSY spectra were collected as $27^{*}(t_1)\times 27^{*}(t_2)\times 768^{*}(t_3)$ data sets (where n* refers to the number of complex data points), with acquisition times of 32.4 ms (t_1), 32.4 ms (t_2), and 82.9 ms (t_3). Data processing was carried out with the NMRPipe package (Delaglio et al., 1995) and peak positions and intensities were determined using the program PIPP (Garrett et al., 1991).

Figure 2 shows ^{15}N strips for ubiquitin extracted from an experiment carried out with a total measuring time of 12 h at 25 °C. Ratios of the cross-peak to diagonal-peak intensities shown in Fig. 2 correspond to values of $^{3}J_{NiNi+1}$ of 0.25 to 0.35 Hz. Despite the low values of the coupling constants, about 70% of the expected interresidue ^{15}N-^{15}N connectivities could be observed as originating or ending on the neighboring residue in the 12 h experiment. When the experiment was carried out with 60 h total measuring time, this percentage increased to 84%. Therefore, the experiment might provide valuable sequential assignment information for smaller proteins that are only available in ^{15}N-labeled form.

A total of four experiments were collected at 25 °C with TOCSY mixing times/total experimental times of 0.25 s/12 h, 0.25 s/12 h, 0.33 s/12 h, and 0.25 s/60 h. For all experiments, J-couplings were determined according to Eq. 2. Figure 3 shows these J-couplings as averages determined from the individual experiments. The rms pairwise difference for 45 nonterminal $^{3}J_{NN}$ values in two 12 h measurements was 0.018 Hz, indicating a random error of 0.013 Hz in the individual values. Upper limits for the J-couplings were derived for cases where one or both of the $^{15}N^{i}$ to $^{15}N^{i+1}$ and $^{15}N^{i+1}$ to $^{15}N^{i}$ correlations were below the detection limit, but both diagonal peaks were clearly observable. This limit is given by the J-coupling that corresponds to an intensity ratio of $(\lambda^2/(I_{ii}*I_{i+1,i+1}))^{1/2}$ in Eq. 2, and λ is set to the intensity of the lowest contour in the peak-picking program. The upper limits are depicted as error bars without a central filled dot. All data are shown as a function of the backbone angle ψ derived from a 1.8 Å crystal structure (Vijay-Kumar et al., 1987).

Most remarkable is the spread of the measured values of J-coupling constants for very similar ψ angles (see Fig. 3). This spread has no obvious correlation to either residue type, mobility, or secondary structure and is very large compared to the reproducibility of the measurement of the individual J-couplings. For example, residue H68 has a ψ angle of 136° and a $^{3}J_{NN}$ value of 0.158 Hz, whereas residue K63 has a ψ angle of 143° and a $^{3}J_{NN}$ value of 0.355 Hz. These deviations are in clear contrast to what is expected from a sole dependence of $^{3}J_{NN}$ on the backbone angle ψ. A linear least squares fit according to the classical Karplus parametrization is shown as a solid line in Fig. 3 ($^{3}J_{NN}/\mathrm{Hz} = -0.013\cos^2\psi - 0.096\cos\psi + 0.174$). In contrast to the usual dependence on the dihedral angle, the fitted curve shows no second maximum for a ψ angle of 0°. According to Eq. 1 the sign of the couplings cannot be determined in quantitative J-correlation experiments.

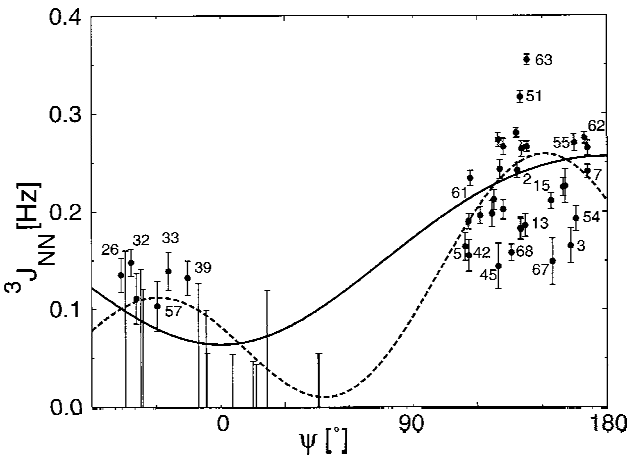

Fig. 3. Relation between the averaged $^{3}J_{NiNi+1}$ couplings of four individual experiments at 25 °C and the backbone ψ angles derived from the crystal structure of human ubiquitin (Vijay-Kumar et al., 1987). Error bars correspond to propagated errors derived from the noise of the individual experiments. In cases where one or both of the $^{15}N^{i}$ to $^{15}N^{i+1}$ and $^{15}N^{i+1}$ to $^{15}N^{i}$ correlations were below the detection limit, upper limits for the J-couplings were derived according to the procedure described in the text. These upper limits are shown as error bars without a central filled dot. The solid and dashed lines represent a tentative Karplus relation according to a least squares fit (see text). J-couplings in less crowded regions are marked by the residue number.

Relative signs are usually derived from the smoothness of the functional dependence on the dihedral angle. Changing the sign of the coupling constants in the region of $\psi < 60°$, however, does not lead to a second maximum in the cis-conformation because the absolute values of the coupling constants for $0° < \psi < 60°$ are considerably smaller than those for $-60° < \psi < 0°$. Substituent effects cause similar asymmetries and a corresponding phase shift in Karplus relations for sp^3-sp^3 fragments (Booth, 1965; Pachler, 1971; Altona, 1996). Indeed, a four-parameter fit according to $^3J_{NN}/Hz = 0.180\cos^2(\psi - 29°) - 0.073\cos(\psi - 29°) + 0.012$ (Fig. 3, dashed line) yields a statistically significant reduction in the reduced χ^2 (from 25.32, 47 degrees of freedom to 22.71, 46 degrees of freedom) and a second maximum in the ψ-dependence. However, given the large deviations of J-values for very similar ψ-angles, this result must be interpreted with great caution.

In order to exclude systematic errors as a cause for this unusual behavior, a detailed error analysis was initiated. One possible source is the finite band width of the DIPSI-2 excitation scheme, which could lead to incomplete transfer. However, changing the ^{15}N carrier position from the center of the amide region at 118 ppm to 122.5 ppm did not alter the measured J-couplings by more than 0.01 Hz, even in cases where the resonance frequencies of the involved ^{15}N nuclei are at the edge of the observed amide chemical shift range. This is in agreement with the expected theoretical efficiency of the DIPSI-2 mixing scheme applied at an rf field strength of 2.8 kHz (Shaka et al., 1988).

More serious sources of error are the relaxation mechanisms which have been neglected in the derivation of Eq. 1: (i) scalar relaxation of the second kind caused by the finite T_1 of either N^j or N^i in the $N^i_x N^j_z$ and $N^j_x N^i_z$ terms involved in the isotropic mixing process (Ernst et al., 1987); (ii) interference between the CSA interaction of $^{15}N^i$ and the $^1H^i$-$^{15}N^i$ dipolar interaction (Goldman, 1984); (iii) interference between the CSA interaction of $^{15}N^i$ and the CSA interaction of $^{15}N^j$; (iv) interference between the CSA interaction of $^{15}N^i$ and the $^1H^j$-$^{15}N^j$ dipolar interaction; and (v) interference between the $^1H^i$-$^{15}N^i$ dipolar interaction and the $^1H^j$-$^{15}N^j$ dipolar interaction.

A straightforward calculation for mechanism (i), which is analogous to the one for COSY mixing (Kuboniwa et al., 1994), shows that the intensity ratio of cross peaks and diagonal peaks including a uniform T_1 for both residues is given by:

$$[(I_{ji} \times I_{ij}) / (I_{ii} \times I_{jj})]^{1/2} = (1 - \zeta)/(1 + \zeta) \qquad (3a)$$

with

$$\zeta = \exp(-\tau_m/(2T_1))[\cos(J_r\tau_m) + \sin(J_r\tau_m)/(2J_rT_1)] \qquad (3b)$$

and a reduced J_r of

$$J_r = [(2\pi J_{NN})^2 - (4T_1)^{-2}]^{1/2} \qquad (3c)$$

In the limit of $J_r\tau_m$, $\tau_m/(4T_1) \ll 1$, these formulas show that the neglect of T_1 leads to a uniform underestimation of the J-values in Eq. 1 by 10% for $\tau_m = 0.33$ s and $T_1 = 0.5$ s, which is a value close to the one determined for most of the non-mobile residues in ubiquitin at 27 °C (Tjandra et al., 1995). Moreover, since the reported ^{15}N T_1 values are very uniform for these residues in ubiquitin, this relaxation mechanism can be excluded as a source of the observed spread in $^3J_{NN}$.

Mechanism (ii): cross-correlation between $^{15}N^i$ CSA and $^1H^i$-$^{15}N^i$ dipolar interactions causes the $^{15}N_i$ nucleus to relax at a different rate, depending on whether it is attached to a $^1H^i$ proton in the $|\alpha\rangle$ or in the $|\beta\rangle$ state (Goldman, 1984). This difference in relaxation rates η is dominated by a term proportional to $J(0)$, where $J(\omega)$ is the spectral density at frequency ω (see e.g. Tjandra et al., 1996). For the non-mobile residues of ubiquitin at 27 °C, η is rather uniform with values of about 3.8 Hz, whereas the average ^{15}N transverse relaxation rates, ρ_2, are about 5.9 Hz (Tjandra et al., 1996). A series of 180° proton pulses (Fig. 1) is applied during the mixing scheme at a rate that is fast compared to η. This intermixes the proton $|\alpha\rangle$ and $|\beta\rangle$ states rapidly, such that the two doublet components decay at the average rate ρ_2 (Boyd et al., 1990; Kay et al., 1992). Omission of the proton intermixing pulses leads to a significant build-up of antiphase N_xH_z magnetization at the end of the mixing period. The four spin modes $\Sigma_x = N^i_x + N^j_x$, $\Delta_x = N^i_x - N^j_x$, $\Sigma_{yz} = 2(N^i_y N^j_z + N^i_z N^j_y)$, $\Delta_{yz} = 2(N^i_y N^j_z - N^i_z N^j_y)$ are commonly used as bases for the density matrix ρ during the isotropic mixing (Ernst et al., 1987). A complete description of relaxation mechanism (ii) during the mixing period can be achieved when the spin mode basis is augmented by the inclusion of the α- and β-states of protons H^i and H^j, such that: $\Sigma_{x\gamma\delta} = \Sigma_x H^i_\gamma H^j_\delta$, $\Delta_{x\gamma\delta} = \Delta_x H^i_\gamma H^j_\delta$, $\Sigma_{yz\gamma\delta} = \Sigma_{yz} H^i_\gamma H^j_\delta$, $\Delta_{yz\gamma\delta} = \Delta_{yz} H^i_\gamma H^j_\delta$, with $\gamma, \delta = \alpha$ or β. Relaxation mechanism (ii) leads to interconversion between the $\Sigma_{x\alpha\beta}$ and $\Delta_{x\alpha\beta}$ modes because the relaxation rates for $N^i_x H^i_\alpha H^j_\beta$ and $N^j_x H^i_\alpha H^j_\beta$ magnetization differ by the value η. No such interconversion occurs between the $\Sigma_{yz\alpha\beta}$ and $\Delta_{yz\alpha\beta}$ spin modes because the DIPSI mixing sequence rotates the ^{15}N spins around the x-axis. This rapidly interconverts the $N^i_y N^j_z H^i_\alpha H^j_\beta$ and $N^i_z N^j_y H^i_\alpha H^j_\beta$ spin states such that they relax at an average rate. The same argument holds for the corresponding $H^i_\beta H^j_\alpha$ expressions. The interconversion between the Σ_x and Δ_x spin modes is reflected in a lower ratio of cross-peak to diagonal-peak intensities of the (H)NNH-TOCSY experiment. A simulation of this effect for a mixing time of 0.33 s and the ρ_2 and η values for ubiquitin shows that this causes a uniform underestimation of the J-values of 4%. Experimentally, a reduction of 5% in J-values was observed when the proton pulses were omitted.

Relaxation mechanisms (iii)–(v) are interference effects

between CSA/CSA, CSA/dipolar, and dipolar/dipolar interactions involving the ^1H-^{15}N pairs of different amino acids i and j. The description of each of these effects by the Redfield theory (Redfield, 1965) is very similar, since the double commutator terms relevant for the description of the TOCSY mixing scheme all involve cross products between the N^i_+ and N^j_- operators. Therefore, the relaxation rates of these mechanisms are all proportional to $J(\omega_N)$. In particular, the spin operator terms defining the Redfield matrix are: $[N^i_+,[N^j_-,\rho]]$ (iii), $[H^i_zN^i_+,[N^j_-,\rho]]$ and $[N^i_+,[H^j_zN^j_-,\rho]]$ (iv), and $[H^i_zN^i_+,[H^j_zN^j_-,\rho]]$ (v), as well as their complex adjoints. Similar to mechanism (ii), mechanisms (iv) and (v) involve operators containing H^i_z and H^j_z and a complete description of relaxation during the mixing scheme can be achieved with the spin modes $\Sigma_{x\gamma\delta}$, $\Delta_{x\gamma\delta}$, $\Sigma_{yz\gamma\delta}$, and $\Delta_{yz\gamma\delta}$. Simple commutator algebra shows that of these four terms only $\Sigma_{yz\gamma\delta}$ and $\Delta_{yz\gamma\delta}$ do not vanish after the application of the double commutators and that they are eigenvectors of the Redfield matrix. Relaxation rates of the operator products $\Sigma_{yz\gamma\delta}$ and $\Delta_{yz\gamma\delta}$ for the different mechanisms are:

$$k_{CSAiCSAj}(\Sigma_{yz\gamma\delta}) = -k_{CSAiCSAj}(\Delta_{yz\gamma\delta}) = 3/10\, c_i c_j\, J(\omega_N)\, P_2(\cos\Theta_{CSAiCSAj}) \quad (4a)$$

$$k_{CSAiDIPj}(\Sigma_{yz\gamma\delta}) = -k_{CSAiDIPj}(\Delta_{yz\gamma\delta}) = -3/10\, c_i d_{HN}\, (2\delta_{\delta\alpha} - 1) J(\omega_N)\, P_2(\cos\Theta_{CSAiDIPj}) \quad (4b)$$

$$k_{DIPiCSAj}(\Sigma_{yz\gamma\delta}) = -k_{DIPiCSAj}(\Delta_{yz\gamma\delta}) = -3/10\, c_j d_{HN}\, (2\delta_{\gamma\alpha} - 1) J(\omega_N)\, P_2(\cos\Theta_{DIPiCSAj}) \quad (4c)$$

$$k_{DIPiDIPj}(\Sigma_{yz\gamma\delta}) = -k_{DIPiDIPj}(\Delta_{yz\gamma\delta}) = 3/10\, d^2_{HN}\, (2\delta_{\gamma\delta} - 1) J(\omega_N)\, P_2(\cos\Theta_{DIPiDIPj}) \quad (4d)$$

with $c_i = 2(\sigma^i_\parallel - \sigma^i_\perp)\omega_N B_o/3$; $d_{HN} = h\gamma_H\gamma_N/(2\pi r^3_{HN})$; $J(\omega_N) = \tau/(1 + \omega^2_N\tau^2)$; $\delta_{\alpha\beta} = 1$, if $\alpha = \beta$, and 0 otherwise; $P_2(x) = (3x^2 - 1)/2$ and Θ the angle between the unique axes of the two interactions involved. Assuming that $\sigma^i_\parallel - \sigma^i_\perp = -160$ ppm, $r_{HN} = 1.02$ Å, $\tau = 4$ ns, $\omega_N = 2\pi$ 60 MHz, and $\cos\Theta = 1$, calculated values for the rate constants are: $k_{CSAiCSAj}(\Sigma_{yz\gamma\delta}) = 0.6$ Hz, $k_{CSAiDIPj}(\Sigma_{yz\gamma\delta}) = (2\delta_{\delta\alpha} - 1) * 1.1$ Hz, $k_{DIPiCSAj}(\Sigma_{yz\gamma\delta}) = (2\delta_{\gamma\alpha} - 1) * 1.1$ Hz, and $k_{DIPiDIPj}(\Sigma_{yz\gamma\delta}) = (2\delta_{\gamma\delta} - 1) * 1.9$ Hz. Numerical simulations show that the combination of all these relaxation mechanisms leads to a maximal error of 13% for the ratios of cross-peak to diagonal-peak intensities, resulting in a maximal error of 7% in the determination of the J-couplings for a mixing time of 0.33 s. We therefore conclude that the relaxation mechanisms (i–v) are not a possible source of the variations observed in Fig. 3.

This theoretical conclusion is corroborated by the experimental observation that the values of the $^3J_{NN}$ determined with the (H)NNH-TOCSY sequence do not change significantly with temperature. Figure 4 shows the correlation of $^3J_{NN}$ determined at 45 °C versus $^3J_{NN}$ determined at 25 °C. The rms pairwise difference between the two data sets for 30 nonterminal $^3J_{NN}$ values is only 0.016 Hz, i.e. very similar to the rms difference of two data sets measured at the same temperature. The rotational correlation time of ubiquitin changes from ~4.3 ns to ~2.9 ns when the temperature is increased from 25 °C to 45 °C. If relaxation or motional averaging had a significant influence on $^3J_{NN}$ determined with the (H)NNH-TOCSY, more dramatic systematic changes in J-values would have been induced by the temperature change.

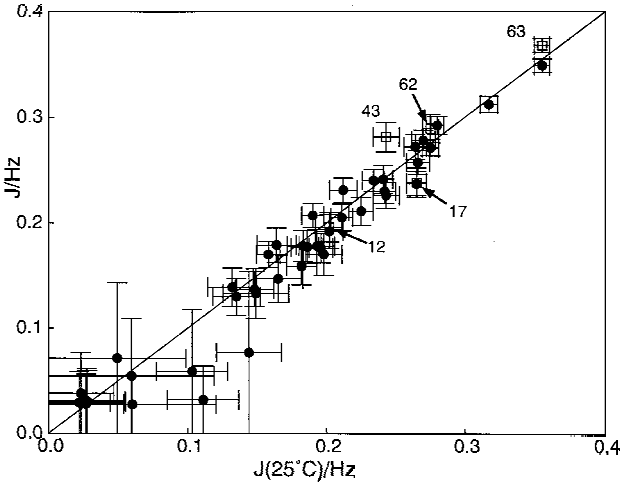

Fig. 4. Comparison of $^3J_{NiNi+1}$ couplings determined at two different temperatures and in D_2O or H_2O. Solid dots show data obtained from the (H)NNH-TOCSY experiment at 45 °C (vertical axis, 12 h total measuring time) and the averaged $^3J_{NiNi+1}$ couplings determined at 25 °C (horizontal axis). Error bars correspond to propagated errors determined from the noise level of the individual experiments. Open squares mark data from an HA(CACO)N-TOCSY experiment (see text) carried out in D_2O (vertical axis, 25 °C, 60 h total measuring time) as compared to the $^3J_{NiNi+1}$ values determined from the (H)NNH-TOCSY experiment carried out in H_2O (25 °C). The numbering corresponds to the residue numbers of human ubiquitin.

The scheme of Fig. 1 is best carried out on a protein sample with uniform ^{15}N enrichment in H_2O. Alternatively, similar information could be derived from a scheme (not shown) which is based on a deuterium-decoupled HA(CACO)N experiment (Wang et al., 1995) carried out on a sample with uniform ^{13}C and ^{15}N enrichment in D_2O. In this pulse sequence, the ^{15}N evolution period of the original experiment (Wang et al., 1995) has to be replaced by a ^{15}N-TOCSY sequence preceded and followed by two ^{15}N semi-constant time evolution periods. The sensitivity of this experiment benefits to some extent from the dramatically increased relaxation time of the ^{15}N nucleus bonded to $^2H^N$ (Wang et al., 1995). However, relaxation losses during the rest of the magnetization transfer and detection periods make this experiment about four times lower in sensitivity than the scheme of Fig. 1 for samples of human ubiquitin at 25 °C (data not shown). The results

of this HA(CACO)N-DIPSI experiment were however included into Fig. 4 in order to show that the replacement of $^1H^N$ by $^2H^N$ has no significant influence on the value of $^3J_{NN}$. For the five residues for which both i to i+1 and i+1 to i cross peaks could be observed, the rms pairwise difference to the averaged (H)NNH-TOCSY data set is 0.022 Hz.

In summary, we conclude that statistical or systematic errors cannot explain the observed variations of $^3J_{NN}$ for very similar ψ angles in human ubiquitin. Similarly, these variations are not correlated to differences in the local mobility of the respective residues (Tjandra et al., 1995). Thus, these variations probably reflect true differences in the electronic wave functions that transmit the nuclear polarization between nuclei $^{15}N^i$ and $^{15}N^j$. The deviations from a unique dependence on the ψ angle are most pronounced for large ψ angles. Of the ordered residues of ubiquitin for which $^3J_{NN}$ couplings were observable in the (H)NNH-TOCSY experiment (2–71), 35 residues have ψ angles larger than 90°. According to the program PROCHECK (Laskowski et al., 1993), eight of these 35 residues (3, 5, 13, 15, 42, 61, 67, and 68) show deviations in the main-chain bond lengths or bond angles from mean values of small molecule data that are larger than three standard deviations. Many of these residues have $^3J_{NiNi+1}$-couplings which are significantly lower than the J-values found for other residues with similar ψ angles (Fig. 3). Distortions from an ideal covalent geometry are, however, not observed for the two residues (E51 and K63) which have significantly increased $^3J_{NiNi+1}$-couplings.

The measured $^3J_{NN}$-couplings are considerably smaller than any of the previously determined three-bond J-couplings in proteins, and similar deviations from a Karplus behavior have not been observed for any other protein three-bond J-couplings. Possible causes for these deviations are substituent effects (Booth, 1965), the effect of the nitrogen lone pair (Gopinathan and Narashiman, 1971) or other electronic interactions which could become dominant at this small absolute size of the scalar couplings.

Acknowledgements

We thank Dennis Torchia and Ad Bax for helpful discussions and Prof. Georg Büldt for encouragement and continuous support. We also thank the referees for their valuable suggestions.

References

Altona, C. (1996) In *Encyclopedia of Nuclear Magnetic Resonance* (Editors-in-Chief, Grant, D.M. and Harris, R.K.), Vol. 4, Wiley, London, U.K., pp. 4909–4923.

Bax, A. and Davis, D.G. (1985) *J. Magn. Reson.*, **65**, 355–360.

Boyd, J., Hommel, U. and Campbell, I.D. (1990) *Chem. Phys. Lett.*, **175**, 477–482.

Booth, H. (1965) *Tetrahedron Lett.*, 411–416.

Braunschweiler, L. and Ernst, R.R. (1983) *J. Magn. Reson.*, **53**, 521–528.

Bystrov, V.F. (1976) *Prog. NMR Spectrosc.*, **10**, 41–81.

Delaglio, F., Grzesiek, S., Vuister, G.W., Zhu, G., Pfeifer, J. and Bax, A. (1995) *J. Biomol. NMR*, **6**, 277–293.

DeMarco, A., Llinás, M. and Wüthrich, K. (1978) *Biopolymers*, **17**, 2727–2742.

Ernst, R.R., Bodenhausen, G. and Wokaun, A. (1987) *Principles of Nuclear Magnetic Resonance in One and Two Dimensions*, Clarendon Press, Oxford, U.K., p. 445.

Garrett, D.S., Powers, R., Gronenborn, A.M. and Clore, G.M. (1991) *J. Magn. Reson.*, **95**, 214–220.

Garrett, D.S., Kuszewski, J., Hancock, T.J., Lodi, P.J., Vuister, G.W., Gronenborn, A.M. and Clore, G.M. (1994) *J. Magn. Reson.*, **B104**, 99–103.

Goldman, M. (1984) *J. Magn. Reson.*, **60**, 437–452.

Gopinathan, M.S. and Narashiman, P.T. (1971) *Mol. Phys.*, **22**, 473–481.

Grzesiek, S. and Bax, A. (1997) *J. Biomol. NMR*, **9**, 207–211.

Hu, J.-S. and Bax, A. (1996) *J. Am. Chem. Soc.*, **118**, 8170–8171.

Kay, L.E., Nicholson, L.K., Delaglio, F., Bax, A. and Torchia, D.A. (1992) *J. Magn. Reson.*, **97**, 359–375.

Kuboniwa, H., Grzesiek, S., Delaglio, F. and Bax, A. (1994) *J. Biomol. NMR*, **4**, 871–878.

Laskowski, R.A., MacArthur, M.W., Moss, D.S. and Thornton, J.M. (1993) *J. Appl. Crystallogr.*, **26**, 283–291.

Ludvigsen, S., Andersen, K.V. and Poulsen, F.M. (1991) *J. Mol. Biol.*, **217**, 731–736.

Pachler, K.G.R. (1971) *Tetrahedron*, **27**, 187–199.

Pardi, A., Billeter, M. and Wüthrich, K. (1984) *J. Mol. Biol.*, **180**, 741–751.

Redfield, A.G. (1965) *Adv. Magn. Reson.*, **1**, 1–32.

Schleucher, J., Quant, J., Glaser, S.J. and Griesinger, C. (1996) In *Encyclopedia of Nuclear Magnetic Resonance* (Editors-in-Chief, Grant, D.M. and Harris, R.K.), Vol. 6, Wiley, London., U.K., pp. 4789–4804.

Schmieder, P., Thanabal, V., McIntosh, L.P., Dahlquist, F.W. and Wagner, G. (1992) *J. Am. Chem. Soc.*, **113**, 6323–6324.

Seip, S., Balbach, J. and Kessler, H. (1994) *J. Magn. Reson.*, **B104**, 172–179.

Shaka, A.J., Lee, C.J. and Pines, A. (1988) *J. Magn. Reson.*, **77**, 274–293.

Tjandra, N., Feller, S.E., Pastor, R.W. and Bax, A. (1995) *J. Am. Chem. Soc.*, **117**, 12562–12566.

Tjandra, N., Szabo, A. and Bax, A. (1996) *J. Am. Chem. Soc.*, **118**, 6986–6991.

Vijay-Kumar, S., Bugg, C.E. and Cook, W.J. (1987) *J. Mol. Biol.*, **194**, 531–544.

Wang, A.C. and Bax, A. (1995) *J. Am. Chem. Soc.*, **117**, 1810–1813.

Wang, A.C., Grzesiek, S., Tschudin, R., Lodi, P.J. and Bax, A. (1995) *J. Biomol. NMR*, **5**, 376–382.

Wang, A.C. and Bax, A. (1996) *J. Am. Chem. Soc.*, **118**, 2483–2494.

Weisemann, R., Löhr, F. and Rüterjans, H. (1994) *J. Biomol. NMR*, **4**, 587–593.

Wüthrich, K. (1986) *NMR of Proteins and Nucleic Acids*, Wiley, New York, NY, U.S.A.